

# Nonlinear hydroelastic waves traveling in a thin elastic plate floating on a two-layer fluid



P. Wang<sup>a,b</sup>, D.Q. Lu<sup>a,c,\*</sup>

<sup>a</sup> Shanghai Institute of Applied Mathematics and Mechanics, Shanghai University, Yanchang Road, Shanghai 200072, China

<sup>b</sup> School of Mathematics and Physics, Qingdao University of Science and Technology, Songling Road, Qingdao 266061, China

<sup>c</sup> Shanghai Key Laboratory of Mechanics in Energy Engineering, Yanchang Road, Shanghai 200072, China

## ARTICLE INFO

### Keywords:

Two-layer fluid  
Nonlinear progressive waves  
Elastic plate  
Homotopy analysis method (HAM)

## ABSTRACT

Effects of the sharp stratification of fluid density on the nonlinear hydroelastic waves traveling in an infinite elastic plate floating on a two-layer inviscid fluid are analytically investigated with the aid of the homotopy analysis method. Under the assumptions that the upper and lower fluid layers with different constant densities are incompressible and the motion is irrotational, the problem is formulated within the frame of the potential flow theory. The convergent series solutions for the velocity potentials, the plate deflection and the interfacial elevation are derived, from which the interaction between surface hydroelastic waves and interfacial gravity waves is studied. The influences of different physical parameters, including the density ratio and the depth ratio of the fluid layers, Young's modulus and the thickness of the plate on the progressive waves are discussed. It is found that the increment of those plate parameters has slight influence on the interfacial wave elevation and apparently changes the plate deflection. A larger density ratio or depth ratio of the fluid layers can reduce the plate deflection and the interfacial wave elevation.

© 2015 Elsevier Inc. All rights reserved.

## 1. Introduction

Investigation on hydroelastic interaction between the water waves and very large floating structures (VLFSs), which are intended for storage facilities, floating airports and even mobile offshore bases, has gained considerable attention under the rapidly growing demand for exploiting ocean resources and making great use of marine space. Due to their large horizontal scale and small bending rigidity, the new-style structures are mathematically idealized as thin elastic plates or beams. So the design of a safe and economic VLFS relies on the accurate estimation and full understanding of its elastic deformation [1–6]. Studies on wave-plate interaction are of great importance for practical application and theoretical interest. Coincidentally, these models are available to analyze the large floating ice sheets and floes in the polar region [7–12].

As it is well known, the real ocean may emerge a stratification phenomenon due to the vertical variation of water temperature, salinity and density. Some researchers employed a two-layer fluid model to describe the stratified ocean in the scope of linear theory. Linton and McIver [13] proposed a two-dimensional linear scattering theory to investigate the interaction between water waves and horizontal cylinders in a two-layer fluid. Recently, Xu and Lu [14] adopted the inner product method to discuss the wave scattering by the semi-infinite or finite elastic plates floating on a two-layer fluid, and studied the effects of the fluid density

\* Corresponding author. fax.: +86 21 56338372; fax +86 21 36033287.

E-mail address: [dqlu@graduate.hku.hk](mailto:dqlu@graduate.hku.hk), [dqlu@shu.edu.cn](mailto:dqlu@shu.edu.cn) (D.Q. Lu).

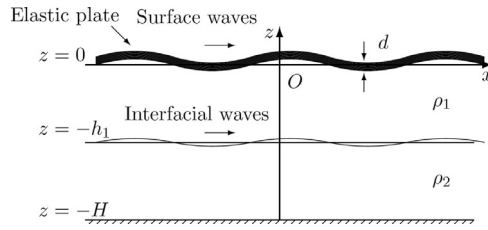


Fig. 1. Coordinates

ratio and the position of interface on the wave reflection and transmission. Lin and Lu [15] studied hydroelastic interaction between obliquely incident waves and a semi-infinite elastic plate on a two-layer fluid, and obtained three critical angles for the incident waves of the interfacial wave mode and one critical angle for the incident waves of the surface wave mode. Moreover, Lin and Lu [16] investigated the water wave diffraction by a bottom-mounted circular cylinder clamped to an elastic plate floating on a two-layer fluid of finite depth. And discussed the horizontal forces and the moments exerted on the circular cylinder due to different wave modes. It is shown that the evanescent wave modes are appreciable parts for a high frequency.

In the last two decades, the homotopy analysis method (HAM), which does not rely on any small or large parameters [17–19], has successfully been introduced to solve analytically some highly nonlinear hydrodynamic problems [20–24] and the heat and mass transfer of two-layer flows of a nano-fluids [25]. Recently, Wang and Lu [26] applied the HAM to study nonlinear hydroelastic progressive waves traveling in an infinite elastic plate in infinitely deep fluid. It was shown that several physical parameters have important effects on the hydroelastic response of the floating plate. In this paper, we extend the study for a single layer fluid [26] to the case of a two-layer fluid. Using the HAM in a similar way, we modify the equations of linear sub-problems and solution expressions derived by Wang and Lu [26], and employ the continuities of the velocity and the pressure on the interface between the upper and lower fluids to obtain the relationship between the series solutions for two different fluid layers. It is found that several physical parameters, including Young’s modulus, and the thickness and density of the plate, have analogous effects on the plate deflection for the case with a single layer fluid [26], which confirms that some conclusions for a single fluid also hold for a two-layer fluid. Furthermore, the influences of the density and depth ratios of the two-layer fluid on the plate deflection and the interfacial wave elevation are investigated detailedly.

The mathematical model is formulated in Section 2. In Section 3, we present the solution procedure in the frame of HAM, by which we can transfer the simultaneous nonlinear equations into linear and decoupled sub-problems for a two-layer fluid problem. The results of numerical calculations and the discussion are shown in Section 4. We figure out the values of the convergence-control parameter and the plate deflection for different parameters. Concluding remarks follow in Section 5.

## 2. Mathematical formulation

Nonlinear hydroelastic waves traveling in an infinite elastic thin plate floating on a two-layer fluid of constant depth is considered for the two-dimensional case, as shown in Fig. 1. Cartesian coordinates  $oxz$  are chosen such that the  $x$  axis coincides with the undisturbed upper fluid surface while the  $z$  axis points vertically upward, with  $z = -h_1$  as the fluid interface and  $z = -H$  as the flat rigid seabed. The floating plate with uniform mass density  $\rho_e$  and constant thickness  $d$  extends to the infinity along the  $x$  axis without draft. The elevations of the top surface and the middle interface are denoted by  $\zeta_1(x, t)$  and  $\zeta_2(x, t)$ , respectively. The upper fluid layer with constant density  $\rho_1$  occupies the region  $-h_1 \leq z \leq \zeta_1(x, t)$ , and the lower fluid layer with constant density  $\rho_2$  occupies the region  $-H \leq z \leq -h_1 + \zeta_2(x, t)$ . Under the assumptions that the upper and lower fluids are inviscid and incompressible and that the motion is irrotational, the problem can be described by the potential flow theory. The velocity potentials in the upper and lower fluid layers are denoted by  $\phi_1$  and  $\phi_2$ , respectively, which satisfy the Laplace equation

$$\frac{\partial^2 \phi_n}{\partial x^2} + \frac{\partial^2 \phi_n}{\partial z^2} = 0, \quad (n = 1, 2), \tag{1}$$

in the corresponding region.

With the assumption that there is no cavitation between the fluid and the plate, the surface pressure is equal to the pressure of the plate. Thus, without draft the nonlinear kinematic and dynamic boundary conditions on the fluid-plate interface ( $z = \zeta_1(x, t)$ ) are respectively modeled as

$$\frac{\partial \zeta_1}{\partial t} + \frac{\partial \phi_1}{\partial x} \frac{\partial \zeta_1}{\partial x} = \frac{\partial \phi_1}{\partial z}, \tag{2}$$

$$\frac{\partial \phi_1}{\partial t} + \frac{1}{2} |\nabla \phi_1|^2 + g \zeta_1 + \frac{1}{\rho_1} \left[ D \frac{\partial^4 \zeta_1}{\partial x^4} + m_e \left( \frac{\partial^2 \zeta_1}{\partial t^2} + g \right) \right] = 0, \tag{3}$$

where  $g$  is the gravitational acceleration;  $D$  is the flexural rigidity of the plate, which is expressed as  $D = Ed^3/[12(1 - \nu^2)]$ , by Young’s modulus  $E$ , Poisson’s ratio  $\nu$  and the thickness  $d$  of the plate;  $m_e = \rho_e d$  is the mass per unit area of the plate.

From the kinematic boundary condition and the continuities of the velocity and the pressure on the interface ( $z = -h_1 + \zeta_2(x, t)$ ) between the upper and lower fluids, we have

$$\frac{\partial \zeta_2}{\partial t} + \frac{\partial \phi_2}{\partial x} \frac{\partial \zeta_2}{\partial x} = \frac{\partial \phi_2}{\partial z}, \quad (4)$$

$$\frac{\partial \phi_1}{\partial z} = \frac{\partial \phi_2}{\partial z}, \quad (5)$$

$$\gamma \left( \frac{\partial \phi_1}{\partial t} + \frac{1}{2} |\nabla \phi_1|^2 + g \zeta_2 \right) = \frac{\partial \phi_2}{\partial t} + \frac{1}{2} |\nabla \phi_2|^2 + g \zeta_2, \quad (6)$$

where  $\gamma = \rho_1/\rho_2$  and  $0 < \gamma < 1$ . Additionally, the boundary condition on the flat rigid bottom reads

$$\frac{\partial \phi_2}{\partial z} = 0, \quad (z = -H). \quad (7)$$

Based on the traveling-wave method, we still introduce the same independent variable transformation as Wang and Lu [26]

$$X = kx - \omega t, \quad (8)$$

where  $k$  is the wave number and  $\omega$  is a given angular frequency. For clarity, we nondimensionalized the physical variables as follows

$$\begin{aligned} x^* &= kx, \quad z^* = kz, \quad d^* = kd, \quad \zeta^* = k\zeta, \quad t^* = t(gk)^{\frac{1}{2}}, \quad \omega^* = \omega/(gk)^{\frac{1}{2}}, \quad \phi_n^* = k^2 \phi_n / (gk)^{\frac{1}{2}}, \\ D^* &= k^4 D / (\rho_1 g), \quad E^* = kE / (\rho_1 g), \quad \rho_e^* = \rho_e / \rho_1, \quad m_e^* = km_e / \rho_1. \end{aligned} \quad (9)$$

All the star superscripts are omitted hereinafter for the nondimensional variables.

With the aid of transformation (8), the differential operators  $\partial/\partial t$  and  $\partial/\partial x$  in Eqs. (1)–(7) are changed into  $-\omega \partial/\partial X$  and  $\partial/\partial X$ , respectively, and  $\partial/\partial z$  keeps the same form. For simplicity, we introduce two differential operators  $\mathcal{L}[\cdot]$  and  $\mathcal{S}[\cdot]$  for  $\phi_n(X, z)$  as follows:

$$\mathcal{L}[\phi_n] = \frac{\partial^2 \phi_n}{\partial X^2} + \frac{\partial^2 \phi_n}{\partial z^2}, \quad (10)$$

$$\mathcal{S}[\phi_n] = \frac{1}{2} \left[ \left( \frac{\partial \phi_n}{\partial X} \right)^2 + \left( \frac{\partial \phi_n}{\partial z} \right)^2 \right]. \quad (11)$$

Thus the dimensionless governing equation for the velocity potentials is

$$\mathcal{L}[\phi_n] = 0, \quad (n = 1, 2). \quad (12)$$

By the transformation (8), a combination of Eqs. (2) and (3) on the unknown plate-covered surface ( $z = \zeta_1(X)$ ) reads

$$\omega^2 \frac{\partial^2 \phi_1}{\partial X^2} + \frac{\partial \phi_1}{\partial z} - \omega \frac{\partial f_1}{\partial X} - \frac{\partial \phi_1}{\partial X} \frac{d\zeta_1}{dX} - \omega D \frac{d^5 \zeta_1}{dX^5} - \omega^3 m_e \frac{d^3 \zeta_1}{dX^3} = 0, \quad (13)$$

where  $f_1 = \mathcal{S}[\phi_1]$ . Similarly, on the unknown interface ( $z = -h_1 + \zeta_2(X)$ ), a combination of Eqs. (4) and (6) yields

$$\frac{\omega^2}{\varepsilon} \frac{\partial^2 \phi_2}{\partial X^2} + \frac{\partial \phi_2}{\partial z} - \frac{\gamma \omega}{\varepsilon} \left[ \omega \frac{\partial^2 \phi_1}{\partial X^2} - \frac{\partial f_1}{\partial X} \right] - \frac{\omega}{\varepsilon} \frac{\partial f_2}{\partial X} - \frac{\partial \phi_2}{\partial X} \frac{d\zeta_2}{dX} = 0, \quad (14)$$

where  $\varepsilon = 1 - \gamma$  and  $f_2 = \mathcal{S}[\phi_2]$ . With the transformation (8), Eqs. (3) and (6) are changed into

$$-\omega \frac{\partial \phi_1}{\partial X} + f_1 + \zeta_1 + D \frac{d^4 \zeta_1}{dX^4} + m_e \left( \omega^2 \frac{d^2 \zeta_1}{dX^2} + 1 \right) = 0, \quad (15)$$

$$\zeta_2 = \frac{1}{\varepsilon} \left[ \gamma \left( -\omega \frac{\partial \phi_1}{\partial X} + f_1 \right) + \omega \frac{\partial \phi_2}{\partial X} - f_2 \right], \quad (16)$$

respectively. Now the unknown functions  $\phi_n(X, z)$  and  $\zeta_n(X)$  with  $n = 1, 2$  are governed by Eqs. (12)–(16), (5) and (7). For a given angular frequency  $\omega$ , the convergent analytical series solutions will be obtained based on the HAM in the subsequent sections.

### 3. Analytical approach based on the HAM

#### 3.1. Continuous variations

Let  $q \in [0, 1]$  be an embedding parameter and the non-zero embedding parameter  $c_0$  denote the convergence-control parameter. Instead of solving these nonlinear equations (12)–(16), (5) and (7) directly, we construct, in the frame of the HAM,  $\Phi_n(X, z; q)$  and  $\eta_n(X; q)$  which are called homotopies in topology such that, as  $q$  increases from 0 to 1,  $\Phi_n(X, z; q)$  deforms continuously

from its initial approximation  $\phi_{n,0}(X, z)$  to the exact solution  $\phi_n(X, z)$  of the original problem. This rule also holds for  $\eta_n(X; q)$  from its initial approximation  $\zeta_{n,0}(X)$  to  $\zeta_n(X)$ .

The homotopy  $\Phi_n(X, z; q)$  satisfies the Laplace equations namely  $\mathcal{L}[\Phi_n(X, z; q)] = 0$ , and  $\Phi_2(X, z; q)$  satisfies the bottom boundary condition  $\partial\Phi_n(X, -H; q)/\partial z = 0$ . In addition, the continuous variations  $\Phi_n(X, z; q)$  and  $\eta_n(X; q)$  are governed by a new family of nonlinear partial differential equations (PDEs), namely the zeroth-order deformation equations. For the two boundary conditions on the unknown free surface  $z = \eta_1(X; q)$ , we have

$$(1 - q)\mathcal{L}_{11}[\Phi_1(X, z; q) - \phi_{10}(X, z)] = qc_0\mathcal{N}_{11}[\Phi_1(X, z; q), \eta_1(X; q)], \tag{17}$$

$$(1 - q)\mathcal{L}_{12}[\eta_1(X; q) - \zeta_{10}(X)] = qc_0\mathcal{N}_{12}[\eta_1(X; q), \Phi_1(X, z; q)], \tag{18}$$

where  $\mathcal{L}_{11}[\cdot]$  and  $\mathcal{L}_{12}[\cdot]$  are auxiliary linear operators with  $\mathcal{L}_{11}[0] = \mathcal{L}_{12}[0] = 0$ . According to Eqs. (13) and (15),  $\mathcal{N}_{11}[\cdot, \cdot]$  and  $\mathcal{N}_{12}[\cdot, \cdot]$  are nonlinear differential operators defined by

$$\mathcal{N}_{11}[\Phi_1(X, z; q), \eta_1(X; q)] = \omega^2 \frac{\partial^2 \Phi_1}{\partial X^2} + \frac{\partial \Phi_1}{\partial z} - \omega \frac{\partial F_1}{\partial X} - \frac{\partial \Phi_1}{\partial X} \frac{d\eta_1}{dX} - \omega D \frac{d^5 \eta_1}{dX^5} - \omega^3 m_e \frac{d^3 \eta_1}{dX^3}, \tag{19}$$

$$\mathcal{N}_{12}[\eta_1(X; q), \Phi_1(X, z; q)] = -\omega \frac{\partial \Phi_1}{\partial X} + F_1 + \eta_1 + D \frac{d^4 \eta_1}{dX^4} + m_e \left( \omega^2 \frac{d^2 \eta_1}{dX^2} + 1 \right), \tag{20}$$

respectively, where  $F_1 = \mathcal{S}[\Phi_1(X, z; q)]$ .

For the boundary conditions on the unknown interfacial surface ( $z = -h_1 + \eta_2(X; q)$ ), we have

$$(1 - q)\mathcal{L}_{21}[\Phi_2(X, z; q) - \phi_{20}(X, z)] = qc_0\mathcal{N}_{21}[\Phi_2(X, z; q), \eta_2(X; q)], \tag{21}$$

$$(1 - q)\mathcal{L}_{22}[\eta_2(X; q) - \zeta_{20}(X)] = qc_0\mathcal{N}_{22}[\eta_2(X; q), \Phi_2(X, z; q)], \tag{22}$$

$$\frac{\partial \Phi_1}{\partial z} = \frac{\partial \Phi_2}{\partial z}, \tag{23}$$

where  $\mathcal{L}_{21}[\cdot]$  and  $\mathcal{L}_{22}[\cdot]$  are auxiliary linear operators with  $\mathcal{L}_{21}[0] = \mathcal{L}_{22}[0] = 0$ . According to Eqs. (14) and (16),  $\mathcal{N}_{21}[\cdot, \cdot]$  and  $\mathcal{N}_{22}[\cdot, \cdot]$  are nonlinear differential operators defined by

$$\mathcal{N}_{21}[\Phi_2(X, z; q), \eta_2(X; q)] = \frac{\omega^2}{\varepsilon} \frac{\partial^2 \Phi_2}{\partial X^2} + \frac{\partial \Phi_2}{\partial z} - \frac{\gamma\omega}{\varepsilon} \left[ \omega \frac{\partial^2 \Phi_1}{\partial X^2} - \frac{\partial F_1}{\partial X} \right] - \frac{\omega}{\varepsilon} \frac{\partial F_2}{\partial X} - \frac{\partial \Phi_2}{\partial X} \frac{d\eta_2}{dX}, \tag{24}$$

$$\mathcal{N}_{22}[\eta_2(X; q), \Phi_2(X, z; q)] = \eta_2 - \frac{1}{\varepsilon} \left[ \gamma \left( -\omega \frac{\partial \Phi_1}{\partial X} + F_1 \right) + \omega \frac{\partial \Phi_2}{\partial X} - F_2 \right]. \tag{25}$$

respectively, where  $F_2 = \mathcal{S}[\Phi_2(X, z; q)]$ .

In order to obtain the series solutions for  $\Phi_n(X, z; q)$  and  $\eta_n(X; q)$ , we expand them into the Taylor series about  $q$  at  $q = 0$  as

$$\Phi_n(X, z; q) = \phi_{n,0}(X, z) + \sum_{m=1}^{+\infty} \phi_{n,m}(X, z)q^m, \tag{26}$$

$$\eta_n(X; q) = \zeta_{n,0}(X) + \sum_{m=1}^{+\infty} \zeta_{n,m}(X)q^m, \tag{27}$$

where

$$\{\phi_{n,m}(X, z), \zeta_{n,m}(X)\} = \frac{1}{m!} \frac{\partial^m}{\partial q^m} \{\Phi_n(X, z; q), \eta_n(X; q)\}|_{q=0}. \tag{28}$$

Assuming that  $c_0$  could be so properly chosen that the series in Eqs. (26) and (27) converge at  $q = 1$ , then we have the so called homotopy-series solutions as

$$\phi_n(X, z) = \Phi_n(X, z; 1) = \phi_{n,0}(X, z) + \sum_{m=1}^{+\infty} \phi_{n,m}(X, z), \tag{29}$$

$$\zeta_n(X) = \eta_n(X; 1) = \zeta_{n,0}(X) + \sum_{m=1}^{+\infty} \zeta_{n,m}(X). \tag{30}$$

### 3.2. Solution expressions

Considering that the surface progressive waves propagate periodically in the  $X$  direction with a constant velocity, we may express, from viewpoints of the physical reality, the vertical deflection of the thin plate as

$$\zeta_1(X) = \operatorname{Re} \left[ \sum_{n=0}^{+\infty} A_{1,n} e^{inX} \right], \quad (31)$$

where  $A_{1,n}$  is an unknown coefficient to be determined. According to the linear surface waves theory [14] and the governing equation (12), the potential function  $\phi_1(X, z)$  can be in the form:

$$\phi_1(X, z) = \operatorname{Re} \left[ \sum_{n=1}^{+\infty} \{B_{1,n} \cosh[n(h_1 + z)] + C_{1,n} \sinh[n(h_1 + z)]\} e^{inX} \right], \quad (32)$$

where  $B_{1,n}$  and  $C_{1,n}$  are unknown coefficients to be determined.

We assume that the interfacial progressive waves are still periodic. Then the interfacial wave profile can in the form

$$\zeta_2(X) = \operatorname{Re} \left[ \sum_{n=0}^{+\infty} A_{2,n} e^{inX} \right], \quad (33)$$

where  $A_{2,n}$  is an unknown coefficient. Based on the linear interfacial waves theory [14], the potential function  $\phi_2(X, z)$  is expressed by

$$\phi_2(X, z) = \operatorname{Re} \left[ \sum_{n=1}^{+\infty} B_{2,n} \cosh[n(H + z)] e^{inX} \right], \quad (34)$$

where the unknown coefficient  $B_{2,n} = \csc[n(H - h_1)]C_{1,n}$  is based on the continuity of velocity Eq. (23). It is noted that the potential function  $\phi_2(X, z)$  in Eq. (34) automatically satisfy the governing equation (12) and the bottom condition (7).

Eqs. (31) and (33) are called the solution expressions for the plate deflection and the interfacial wave elevation while Eqs. (32) and (34) for the velocity potentials, which play important roles in the frame of the HAM. As mentioned by Liao [18], in order to simplify greatly the process of solving nonlinear problems, we have extremely large freedom to choose the initial approximations and the auxiliary linear operator. We choose

$$\zeta_{1,0}(X) = \zeta_{2,0}(X) = 0 \quad (35)$$

as the initial guesses for the surface and interfacial wave profiles to simplify the subsequent computation procedure [18]. It should be emphasized that, although the initial guesses are assumed to be zero, the high-order terms can provide the corrections for the homotopy-series solutions due to the nonlinearity inherence in Eqs. (17), (18), (21), and (22). According to the solution expressions (31)–(34), we construct the initial approximations of the potential functions by

$$\phi_{1,0}(X, z) = \operatorname{Re} \{ [B_{1,0} \cosh(h_1 + z) + C_{1,0} \sinh(h_1 + z)] e^{iX} \}, \quad (36)$$

$$\phi_{2,0}(X, z) = \operatorname{Re} [B_{2,0} \cosh(H + z) e^{iX}], \quad (37)$$

respectively, where  $B_{1,0}$  and  $C_{1,0}$  are unknown coefficients and  $B_{2,0} = \csc(H - h_1)C_{1,0}$ .

We choose the auxiliary linear operators for  $\Phi_n(X, z; q)$  in Eqs. (17) and (21) as follows

$$\mathcal{L}_{11}[\Phi_1(X, z; q)] = \omega^2 \frac{\partial^2 \Phi_1}{\partial X^2} + \frac{\partial \Phi_1}{\partial z}, \quad (38)$$

$$\mathcal{L}_{21}[\Phi_2(X, z; q)] = \frac{\omega^2}{\varepsilon} \frac{\partial^2 \Phi_2}{\partial X^2} + \frac{\partial \Phi_2}{\partial z}. \quad (39)$$

We choose the auxiliary linear operators for  $\eta_n(X, z; q)$  in Eqs. (18) and (22) as follows

$$\mathcal{L}_{12}[\eta_1(X; q)] = \frac{\partial^4 \eta_1}{\partial X^4} + \frac{\partial^2 \eta_1}{\partial X^2} + \eta_1, \quad (40)$$

$$\mathcal{L}_{22}[\eta_2(X; q)] = \eta_2. \quad (41)$$

### 3.3. High-order deformation equations

The linear PDEs for the unknown terms  $\phi_{n,m}(X, z)$  and  $\zeta_{n,m}(X)$  can be derived directly from the zeroth-order deformation equations. By differentiating the zero-order deformation equations (17) and (18) for the upper fluid, and Eqs. (21) and (22) for

the lower fluid  $m$  times with respect to  $q$ , then dividing them by  $m!$  and setting  $q = 0$ , we obtain the  $m$ th-order deformation equations for the two-layer fluid

$$\mathcal{L}_{11}[\phi_{1,m}] = c_0 \Delta_{1,m-1}^{\phi_1} + H_m S_{1,m-1} - \bar{S}_{1,m}, \quad (z = 0), \tag{42}$$

$$\mathcal{L}_{12}[\zeta_{1,m}] = c_0 \Delta_{1,m-1}^{\zeta_1} + H_m \left( \frac{\partial^4 \zeta_{1,m-1}}{\partial X^4} + \frac{\partial^2 \zeta_{1,m-1}}{\partial X^2} + \zeta_{1,m-1} \right), \quad (z = 0), \tag{43}$$

$$\mathcal{L}_{21}[\phi_{2,m}] = c_0 \Delta_{2,m-1}^{\phi_1, \phi_2} + H_m S_{2,m-1} - \bar{S}_{2,m}, \quad (z = -h_1), \tag{44}$$

$$\zeta_{2,m} = c_0 \Delta_{2,m-1}^{\zeta_2} + H_m \zeta_{2,m-1}, \quad (z = -h_1), \tag{45}$$

where  $H_m = H(m - 2)$ , and  $H(\cdot)$  is the Heaviside step function. The elaborated expressions for  $\Delta_{1,m-1}^{\phi_1}$ ,  $\Delta_{1,m-1}^{\zeta_1}$ ,  $\Delta_{2,m-1}^{\phi_1, \phi_2}$ ,  $\Delta_{2,m-1}^{\zeta_2}$ ,  $S_{n,m-1}$ , and  $\bar{S}_{n,m}$  are given in [Appendix A](#).

Now we see that the unknown terms  $\phi_{n,m}(X, z)$  and  $\zeta_{n,m}(X)$  are governed by linear PDEs (42)–(45). It should be noted that the sub-problems for these unknown variables are not only linear but also decoupled, and then can be solved easily.

### 3.4. Optimal convergence-control parameters

Even if we fix all physical parameters of the nonlinear problem considered here, there will be still an unknown term  $c_0$  which is used to guarantee the convergence of the HAM-based series solutions. The optimal value of  $c_0$  corresponds to the fastest decrease of the total squared residual  $\varepsilon_m^T$ , which is defined by

$$\varepsilon_m^T = \varepsilon_{1m}^{\phi_1} + \varepsilon_{2m}^{\phi_1, \phi_2} + \sum_{n=1}^2 \varepsilon_{nm}^{\zeta_n}, \tag{46}$$

where

$$\varepsilon_{1m}^{\phi_1} = \frac{1}{(1 + M)^2} \sum_{i=0}^M \left\| \sum_{k=0}^m \Delta_{1k}^{\phi_1}(i\Delta X) \right\|^2, \tag{47}$$

$$\varepsilon_{2m}^{\phi_1, \phi_2} = \frac{1}{(1 + M)^2} \sum_{i=0}^M \left\| \sum_{k=0}^m \Delta_{2k}^{\phi_1, \phi_2}(i\Delta X) \right\|^2, \tag{48}$$

$$\varepsilon_{nm}^{\zeta_n} = \frac{1}{(1 + M)^2} \sum_{i=0}^M \left\| \sum_{k=0}^m \Delta_{nk}^{\zeta_n}(i\Delta X) \right\|^2, \tag{49}$$

$\Delta_{1k}^{\phi_1}$ ,  $\Delta_{2k}^{\phi_1, \phi_2}$  and  $\Delta_{nk}^{\zeta_n}$  are given in [Appendix A](#);  $M$  is the number of the discrete points; and  $\Delta X = \pi/M$ . We choose  $M = 10$  here, and then the optimal convergence control parameter  $c_0$  can be obtained by the minimum of  $\varepsilon_m^T$ .

## 4. Results and discussion

It is noted that, for a given frequency  $\omega$ , the surface and interface progressive waves have different wave numbers, denoted by  $k_1$  and  $k_2$  with  $k_1 \neq k_2$ , respectively. Moreover, the surface and the interface wave motions are coupled, and can influence each other [14–16]. Thus, there are the surface and interfacial wave modes at the surface, so is for the interface. Generally, the dimensional solution expressions (31)–(34) contain two wave modes  $k = k_1$  and  $k = k_2$ . Owing to these physical phenomena, the dimensional case is calculated hereinafter.

To show the validity and accuracy of our HAM-based analytic solutions, the total residual square error  $\varepsilon_m^T$  at different orders is illustrated for the two-layer fluid versus  $c_0$ , as shown in [Fig. 2](#) with the case of  $\omega = 3 \text{ s}^{-1}$ ,  $t = 10\pi \text{ s}$ ,  $h_1 = 0.15 \text{ m}$ ,  $h_1/H = 0.5$ ,  $\rho_e = 0.3 \times 10^{-3} \text{ kg m}^{-3}$ ,  $d = 0.005 \text{ m}$ ,  $E = 10^9 \text{ N m}^{-2}$ ,  $\nu = 0.33$ , and  $\gamma = 0.2$ . We find that, as the order  $m$  increases gradually,  $\varepsilon_m^T$  decreases in the interval  $0 \leq x \leq 0.2$  and the optimal value of  $c_0$  is close to 0.1. Furthermore, [Table 1](#) indicates that, when  $c_0 = 0.1$ , the square error can decrease quickly to  $1.26 \times 10^{-6}$  at the 7th-order approximation. It is demonstrated that our HAM-based solutions for the velocity potentials, the plate deflection and the interfacial wave elevation are highly convergent and accurate.

We consider the effects of several important parameters on the nonlinear hydroelastic waves traveling in a thin elastic plate floating on a two-layer fluid. [Fig. 3](#) shows hydroelastic deflections of the plate and the interfacial wave profiles for different depth ratio  $h_1/H$ . From the comparison between the upper and the lower fluid regions, it is easily found that the amplitudes of the interfacial waves decrease with the increment of the depth ratio.

**Table 1**

The total residual square error  $\epsilon_m^T$  for different approximation order  $m$  with  $c_0 = 0.1$ .

$m$	$\epsilon_m^T$
2	$1.19 \times 10^{-1}$
3	$8.72 \times 10^{-3}$
4	$6.51 \times 10^{-4}$
5	$5.24 \times 10^{-5}$
7	$1.26 \times 10^{-6}$

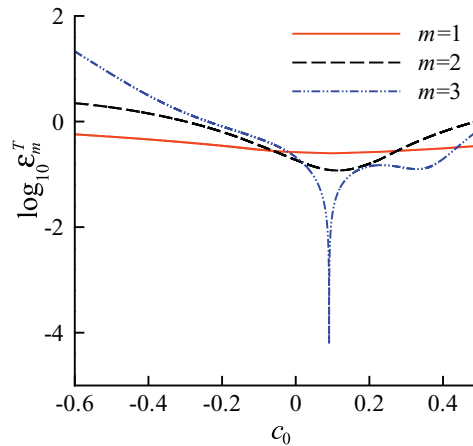


**Fig. 2.** Residual squares of  $\log_{10} \epsilon_m^T$  of the  $m$ th order homotopy approximation for the upper fluid region versus  $c_0$ . Solid line,  $m = 1$ ; long dashed line,  $m = 2$ ; dash-double-dotted line,  $m = 3$ .

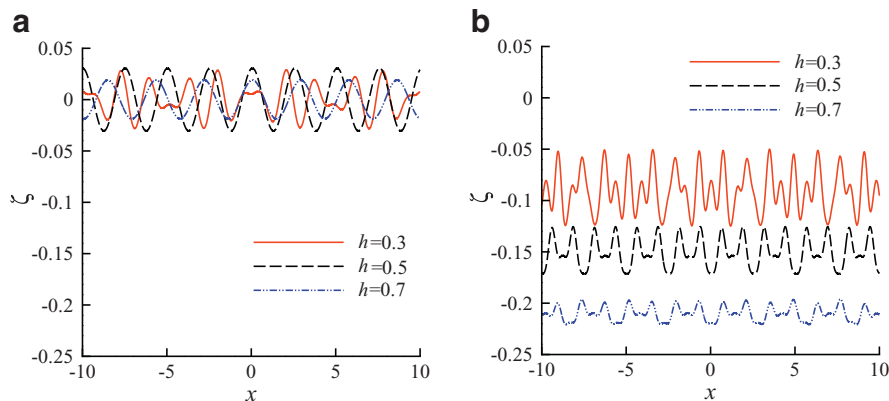


**Fig. 3.** Variation of the plate hydroelastic deflection and the interface wave elevation versus  $x$  for different depth ratio  $h (= h_1/H)$ . (a) The plate deflections. (b) The interfacial waves.

We consider the effects of the density ratio  $\gamma$  on the elastic plate and the interfacial waves by increasing  $\gamma$  from 0.3 to 0.7. It is seen from Fig. 4 that a smaller  $\gamma$  increases the plate deflections and the interfacial wave elevations. The effects of Young's modulus of the plate are shown in Fig. 5, from which we can see that the floating plate's deflections and the interfacial wave elevations decrease with increasing Young's modulus. As Young's modulus increases, the plate deflections become stiffer so that a large reactive force can be generated to resist the elastic deformation of plate. Finally, the effects of the plate thickness  $d$  on the plate deflections and the interfacial waves are studied. Fig. 6 shows that a larger  $d$  flattens the crest and sharpens the trough of the plate deflections and the interfacial waves, which is similar to results for the single-layer fluid. Further, we find that the density ratio  $\gamma$  of the fluid and the Young modulus and the thickness  $d$  of the plate have slight influence on the interfacial wave elevations and apparently changes the surface waves or plate deflections.

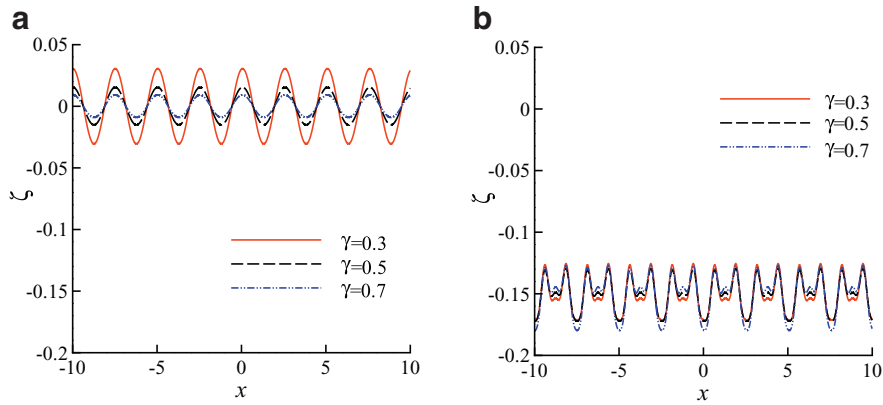


**Fig. 4.** Variation of the plate hydroelastic deflection and the interface wave elevation versus  $x$  for different density ratio  $\gamma$ . (a) The plate deflections. (b) The interfacial waves.

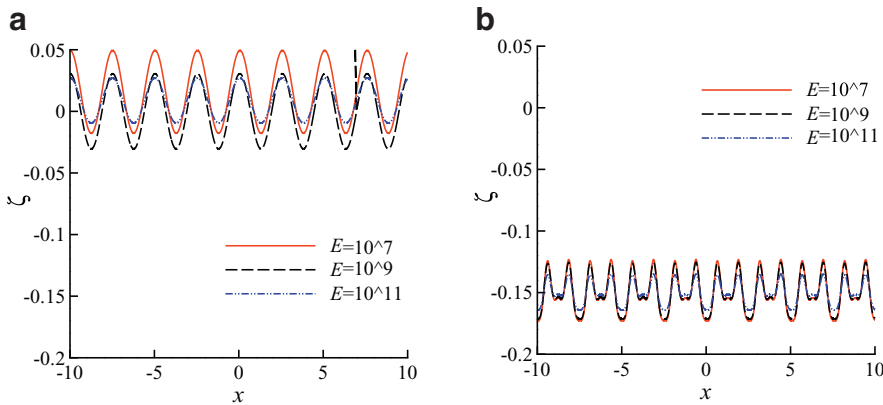


**Fig. 5.** Variation of the plate hydroelastic deflection and the interface wave elevation versus  $x$  for different value of Young's modulus  $E$ . (a) The plate deflections. (b) The interfacial waves.

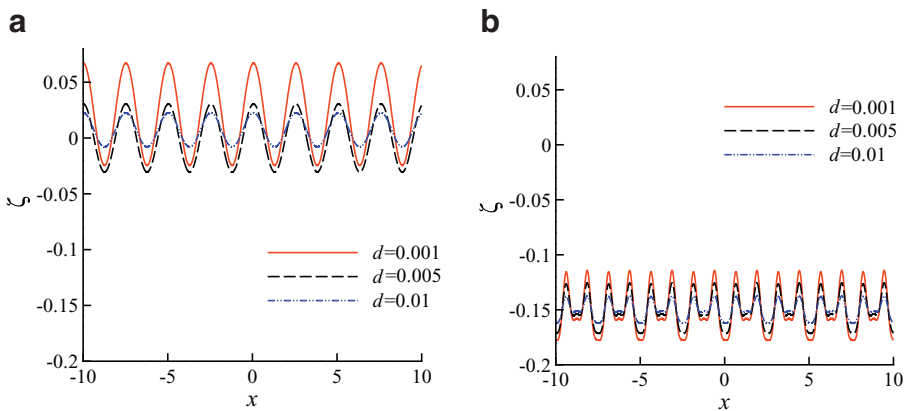


**Fig. 6.** Variation of the plate hydroelastic deflection and the interface wave elevation versus  $x$  for different plate thickness  $d$ . (a) The plate deflections. (b) The interfacial waves.

**5. Conclusions**

We extend the study on nonlinear hydroelastic waves traveling in a single-layer fluid [26] to those in a two-layer fluid of finite depth, which describes the stratification phenomenon of the real ocean. With the help of the HAM, for the whole flow domain including the upper fluid and the lower fluid, the convergent series solutions are analytically derived by solving the simultaneous equations as a boundary-value problem. For simplifying the calculation of nonlinear waves traveling in a thin elastic

plate, we choose the auxiliary linear operators  $\mathcal{L}_{n1}[\cdot]$  containing only the derivatives of  $\phi_n(X, z)$  in nonlinear operators  $\mathcal{N}_{n1}[\cdot, \cdot]$ , and the auxiliary linear operator  $\mathcal{L}_{n2}[\cdot]$  containing only the derivatives of  $\zeta_n(X)$  in nonlinear operators  $\mathcal{N}_{n2}[\cdot, \cdot]$ . Additionally, the relations of those series solutions for two-layer fluid are obtained from the continuities of the velocity and the pressure on the interface between the upper and lower fluids. Numerical results demonstrate the validity and convergence of our HAM-based analytical solutions for the velocity potentials, the plate deflection and the interfacial wave elevation in the two-layer fluid.

The effects of several physical parameters on the nonlinear hydroelastic response of an infinite elastic plate floating on a two-layer fluid are considered in detail. The density and depth ratios of the two-layer fluid, Young's modulus, and the thickness of the plate have some effects on the elastic plate and the interfacial waves. It is found that the larger value of the thickness  $d$ , Young's modulus  $E$  of the plate and the density ratio  $\gamma$  all can flatten the crest, steepen the trough of the plate deflection, and decrease the interfacial wave elevation. With the increment of these parameters, the amplitudes of the interfacial wave decreases slightly while the surface waves decreases significantly. It is found that a larger depth ratio  $h_1/H$  also decreases the amplitudes of the plate deflection and the interfacial waves. All of those results obtained here can help us further understand the nonlinear hydroelastic waves traveling in an elastic plate floating on the stratified ocean.

### Acknowledgments

This research was sponsored by the National Basic Research Program of China under grant no. 2014CB046203, the National Natural Science Foundation of China under grant no. 11472166, the Natural Science Foundation of Shanghai under grant no. 14ZR1416200, and the Natural Science Foundation of Shandong Province of China under grant no. ZR2013AL012.

### Appendix A. Detailed derivations of $\Delta_{1,m-1}^{\phi_1}$ , $\Delta_{1,m-1}^{\zeta_1}$ , $\Delta_{2,m-1}^{\phi_1, \phi_2}$ , $\Delta_{2,m-1}^{\zeta_2}$ , $S_{n,m-1}$ , and $\bar{S}_{n,m}$ ( $n = 1, 2$ ) in Eqs. (42)–(45)

Let

$$(\eta_n)^k = \left( \sum_{i=1}^{+\infty} \zeta_{ni} q^i \right)^k = \sum_{i=k}^{+\infty} \mu_{n,k,i} q^i. \quad (\text{A1})$$

For any  $z$ , we have a Maclaurin series

$$\phi_{nm}(X, z) = \sum_{k=0}^{+\infty} \frac{1}{k!} \left. \frac{\partial^k \phi_{nm}}{\partial z^k} \right|_{z=0} z^k. \quad (\text{A2})$$

For  $z = \eta_n(X; q)$ , it follows from Eqs. (A1) and (A2) that

$$\phi_{nm}(X, \eta_n) = \sum_{k=0}^{+\infty} \left( \frac{1}{k!} \left. \frac{\partial^k \phi_{nm}}{\partial z^k} \right|_{z=0} \right) \left( \sum_{i=k}^{+\infty} \mu_{n,k,i} q^i \right) = \sum_{i=0}^{+\infty} \psi_{n,m,i} q^i, \quad (\text{A3})$$

where

$$\psi_{n,m,i} = \sum_{k=0}^i \left( \frac{1}{k!} \left. \frac{\partial^k \phi_{nm}}{\partial z^k} \right|_{z=0} \right) \mu_{n,k,i}. \quad (\text{A4})$$

Thus we have, for  $z = \eta_n(X; q)$ ,

$$\Phi_n(X, \eta_n; q) = \sum_{m=0}^{+\infty} \phi_{nm}(X, \eta_n) q^m = \sum_{m=0}^{+\infty} \left( \sum_{i=0}^{+\infty} \psi_{n,m,i} q^i \right) q^m = \sum_{m=0}^{+\infty} \varphi_{nm} q^m, \quad (\text{A5})$$

where

$$\varphi_{nm} = \sum_{i=0}^m \psi_{n,m-i}. \quad (\text{A6})$$

Substituting the series expansions (A1) and (A5) into the boundary conditions (17) and (18), then equating the like-power of the embedding parameter  $q$ , we have two linear boundary conditions (42) and (43) for the upper fluid. Similarly, we can have two linear boundary conditions (44) and (45) for the lower fluid. The explicit expressions for  $\Delta_{1,m-1}^{\phi_1}$ ,  $\Delta_{1,m-1}^{\zeta_1}$ ,  $\Delta_{2,m-1}^{\phi_1, \phi_2}$ ,  $\Delta_{2,m-1}^{\zeta_2}$ ,  $S_{n,m-1}$ , and  $\bar{S}_{n,m}$  ( $n = 1, 2$ ) in these conditions are given by

$$\begin{aligned} \Delta_{1,m-1}^{\phi_1} = & \omega^2 \frac{d^2 \varphi_{1,m-1}}{dX^2} + \bar{\varphi}_{1,m-1} - \omega \sum_{k=0}^{m-1} \left( \frac{d\varphi_{1k}}{dX} \frac{d^2 \varphi_{1,m-1-k}}{dX^2} + \bar{\varphi}_{1k} \frac{d\bar{\varphi}_{1,m-1-k}}{dX} \right) \\ & - \omega D \frac{d^3 \zeta_{1,m-1}}{dX^3} - \omega^3 m e \frac{d^3 \zeta_{1,m-1}}{dX^3} - \sum_{k=0}^{m-1} \frac{d\varphi_{1k}}{dX} \frac{d\zeta_{1,m-1-k}}{dX}, \end{aligned} \quad (\text{A7})$$

$$\Delta_{1,m-1}^{\zeta_1} = -\omega \frac{d\varphi_{1,m-1}}{dX} + \frac{1}{2} \sum_{k=0}^{m-1} \left( \frac{d\varphi_{1k}}{dX} \frac{d\varphi_{1,m-1-k}}{dX} + \bar{\varphi}_{1k} \bar{\varphi}_{1,m-1-k} \right) + \zeta_{1,m-1} + D \frac{d^4 \zeta_{1,m-1}}{dX^4} + m e \omega^2 \frac{d^2 \zeta_{1,m-1}}{dX^2}, \quad (m \geq 2), \tag{A8}$$

$$\Delta_{10}^{\zeta_1} = \frac{1}{2} \left[ \left( \frac{d\varphi_{10}}{dX} \right)^2 + (\bar{\varphi}_{10})^2 \right] - \omega \frac{d\varphi_{10}}{dX} + m e, \tag{A9}$$

$$\Delta_{2,m-1}^{\phi_1, \phi_2} = \frac{\omega^2}{1-\gamma} \frac{d^2 \varphi_{2,m-1}}{dX^2} + \bar{\varphi}_{2,m-1} - \frac{\omega}{1-\gamma} \sum_{k=0}^{m-1} \left( \frac{d\varphi_{2k}}{dX} \frac{d\varphi_{2,m-1-k}}{dX^2} + \bar{\varphi}_{2k} \frac{d\bar{\varphi}_{2,m-1-k}}{dX} \right) - \frac{\gamma \omega}{1-\gamma} \left[ \omega \frac{d^2 \varphi_{1,m-1}}{dX^2} - \sum_{k=0}^{m-1} \left( \frac{d\varphi_{1k}}{dX} \frac{d\varphi_{1,m-1-k}}{dX} + \bar{\varphi}_{1k} \bar{\varphi}_{1,m-1-k} \right) \right] - \sum_{k=0}^{m-1} \frac{d\varphi_{2k}}{dX} \frac{d\zeta_{2,m-1-k}}{dX}, \tag{A10}$$

$$\Delta_{2,m-1}^{\zeta_2} = -\frac{1}{1-\gamma} \left\{ \gamma \left[ -\omega \frac{d\varphi_{1,m-1}}{dX} + \frac{1}{2} \sum_{k=0}^{m-1} \left( \frac{d\varphi_{1k}}{dX} \frac{d\varphi_{1,m-1-k}}{dX} + \bar{\varphi}_{1k} \bar{\varphi}_{1,m-1-k} \right) \right] + \zeta_{2,m-1} + \omega \frac{d\varphi_{2,m-1}}{dX} - \frac{1}{2} \sum_{k=0}^{m-1} \left( \frac{d\varphi_{2k}}{dX} \frac{d\varphi_{2,m-1-k}}{dX} + \bar{\varphi}_{2k} \bar{\varphi}_{2,m-1-k} \right) \right\}, \tag{A11}$$

$$S_{n,m-1} = \sum_{i=0}^{m-2} \left( \frac{d^2 \psi_{n,m-1-i,i}}{dX^2} + \gamma_{n,m-1-i,i} \right), \tag{A12}$$

$$\bar{S}_{n,m} = \sum_{i=1}^{m-1} \left( \frac{d^2 \psi_{n,m-i,i}}{dX^2} + \gamma_{n,m-i,i} \right), \tag{A13}$$

where

$$\bar{\varphi}_{n,m-1} = \sum_{i=0}^{m-1} \gamma_{n,m-1-i,i}, \tag{A14}$$

$$\gamma_{n,m-i,i} = \sum_{k=0}^i \frac{1}{k!} \left( \frac{\partial^{k+1} \phi_{n,m-i}}{\partial z^{k+1}} \Big|_{z=0} \right) \mu_{n,k,i}, \quad (n = 1, 2). \tag{A15}$$

**References**

[1] M. Ohkusu, Y. Namba, Hydroelastic analysis of a large floating structure, *J. Fluids Struct.* 19 (4) (2004) 543–555.  
 [2] E. Watanabe, T. Utsunomiya, C. Wang, Hydroelastic analysis of pontoon-type vlf: a literature survey, *Eng. Struct.* 26 (2) (2004) 245–256.  
 [3] S. Ohmatsu, Overview: research on wave loading and responses of vlf, *Mar. Struct.* 18 (2) (2005) 149–168.  
 [4] M. Kashiwagi, Research on hydroelastic responses of VLFs: recent progress and future work, *Int. J. Offshore Polar Eng.* 10 (2) (2000) 81–90.  
 [5] A. Korobkin, E.I. Päräü, J.-M. Vandenberg, The mathematical challenges and modeling of hydroelasticity, *Philos. Trans. Roy. Soc. A: Math. Phys. Eng. Sci.* 369 (2) (2011) 2803–2812.  
 [6] C.M. Wang, Z.Y. Tay, Very large floating structures: applications, research and development, *Procedia Eng.* 14 (2011) 62–72.  
 [7] J. Cheng, S.P. Zhu, S.J. Liao, An explicit series approximation to the optimal exercise boundary of american put options, *Commun. Nonlinear Sci. Numer. Simul.* 15 (5) (2010) 1148–1158.  
 [8] S. Mohapatra, S. Bora, Exciting forces due to interaction of water waves with a submerged sphere in an ice-covered two-layer fluid of finite depth, *Appl. Ocean Res.* 34 (2012) 187–197, doi:10.1016/j.apor.2011.07.008.  
 [9] V.A. Squire, Past, present and independent hydroelastic challenges in the polar and subpolar seas, *Philos. Trans. Roy. Soc. A: Math. Phys. Eng. Sci.* 369 (1947) (2011) 2813–2831.  
 [10] V.A. Squire, Synergies between VLFs hydroelasticity and sea ice research, *Int. J. Offshore Polar Eng.* 18 (4) (2008) 241–253.  
 [11] V.A. Squire, Of ocean waves and sea-ice revisited, *Cold Reg. Sci. Technol.* 49 (2) (2007) 110–133.  
 [12] V.A. Squire, J.P. Dugan, P. Wadhams, P.J. Rottier, A.K. Liu, Of ocean waves and sea ice, *Annu. Rev. Fluid Mech.* 27 (1) (1995) 115–168.  
 [13] C.M. Linton, M. McIver, The interaction of waves with horizontal cylinders in two-layer fluids, *J. Fluid Mech.* 304 (1) (1995) 213–229.  
 [14] F. Xu, D.Q. Lu, Wave scattering by a thin elastic plate floating on a two-layer fluid, *Int. J. Eng. Sci.* 48 (9) (2010) 809–819, doi:10.1016/j.ijengsci.2010.04.007.  
 [15] Q. Lin, D.Q. Lu, Hydroelastic interaction between obliquely incident waves and a semi-infinite elastic plate on a two-layer fluid, *Appl. Ocean Res.* 43 (2013) 71–79.  
 [16] Q. Lin, D.Q. Lu, Water wave diffraction by a bottom-mounted circular cylinder clamped to an elastic plate floating on a two-layer fluid, *Eur. J. Mech.-B/Fluids* 44 (2014) 10–21.  
 [17] S.J. Liao, On the homotopy analysis method for nonlinear problems, *Appl. Math. Comput.* 147 (2) (2004) 499–513.  
 [18] S.J. Liao, *Homotopy Analysis Method in Nonlinear Differential Equations*, Higher Education Press, Beijing, 2012.  
 [19] S.J. Liao, *Beyond Perturbation: Introduction to the Homotopy Analysis Method*, vol. 2, CRC Press, Boca Raton, 2004.  
 [20] J. Cheng, S.Q. Dai, A uniformly valid series solution to the unsteady stagnation-point flow towards an impulsively stretching surface, *Sci. CHINA Phys., Mech. Astron.* 53 (3) (2010) 521–526.  
 [21] S.J. Liao, K.F. Cheung, Homotopy analysis of nonlinear progressive waves in deep water, *J. Eng. Math.* 45 (2) (2003) 105–116.  
 [22] L.B. Tao, H. Song, S. Chakrabarti, Nonlinear progressive waves in water of finite depth – an analytic approximation, *Coast. Eng.* 54 (11) (2007) 825–834.  
 [23] S.J. Liao, On the homotopy multiple-variable method and its applications in the interactions of nonlinear gravity waves, *Commun. Nonlinear Sci. Numer. Simul.* 16 (3) (2011) 1274–1303.

- [24] D.L. Xu, Z.L. Lin, S.J. Liao, M. Stiassnie, On the steady-state fully resonant progressive waves in water of finite depth, *J. Fluid Mech.* 710 (2012) 379–418.
- [25] U. Farooq, T. Hayat, A. Alsaedi, S.J. Liao, Heat and mass transfer of two-layer flows of third-grade nano-fluids in a vertical channel, *Appl. Math. Comput.* 242 (2014) 528–540.
- [26] P. Wang, D.Q. Lu, Analytic approximation to nonlinear hydroelastic waves traveling in a thin elastic plate floating on a fluid, *Sci. China Phys. Mech. Astron.* 56 (11) (2013) 2170–2177.